DOI: 10.1002/adma.200702798

Electrical Detection of Femtomolar DNA via Gold-Nanoparticle Enhancement in Carbon-Nanotube-Network Field-Effect Transistors**

By *Xiaochen Dong, Ching Man Lau, Anup Lohani, Subodh G. Mhaisalkar,* Johnson Kasim, Zexiang Shen, Xinning Ho, John A. Rogers,* and *Lain-Jong Li**

The development of sequence-selective DNA sensors for diagnosis of genetic or pathogenic disease has attracted increasing interest. Most DNA detection methods rely on optical, piezoelectric, or electrochemical transductions. Alternative methods based on the resistance change of a single silicon nanowire or an individual carbon nanotube have been reported. However, these sensors may have significant device-to-device variations and their fabrication requires high production costs. Recently, field-effect transistors (FETs) based on single-walled carbon nanotube (SWNT) networks have been fabricated,[1–4] and their electrical properties depend on the percolation paths of SWNTs in conduction channels, where device variations are expected to be small. Label-free electrical detection of DNA and biomolecules using SWNT network FETs (SNFETs) has been successfully achieved,[5–6] with typical detection limits on the order of ca. 1 nM of DNA. In this Communication, we report that the detection sensitivity of SNFETs for DNA can be further improved to ca. 100 fM by using a ''nanoparticle enhancement'' approach, in which the target DNAs are hybridized with probe DNAs on the device, and reporter DNAs labeled with Au nanoparticles (AuNPs) flank a segment of the target DNA sequence. We note that the enhancement of DNA detection by incorporating nanoparticles (e.g., CdS and Au) has been recently reported by using electrochemical approaches.[7–8] On the other hand, enhancing the sensitivity of SNFETs from 1 nM to 1 pM by adding a bivalent salt ($MgCl_2$) during the hybridization process has also been reported.[5] In some of these approaches, adsorption of target DNA on a SiO_2 surface via divalent coordination (DNA–Mg^{2+}–SiO_2)[9] rather than specific binding cannot be ruled out and may confound the sensing results. We blocked the SiO_2 surface by octyltrichlorosilane (OTS) treatment to reduce possible non-specific binding (NSB) of DNA to SiO_2. In addition, blocking of vacant SWNT surfaces by using polyethylene glycol (PEG; molecular weight 400 kg mol^{-1}) has also been performed to reduce the NSB of DNA to SWNTs.

Figure 1 illustrates the approach taken towards DNA detection enhancement in SNFETs by using reporter DNA–AuNP conjugates. The AuNPs were attached by thiolated reporter DNAs, which were further bound to part of the target DNA strand (in this case, the sequence of the reporter DNA AAAAAA (6A) or AAAAAAAAAAA (11A) matched with the sequence TTTTTTTTTTT of the target DNA). The subsequent hybridization of target DNA brought the AuNPs onto SNFETs through specific binding events. SNFETs (channel lengths: 50, 75, and 100 μm) were fabricated in a top-contact geometry,[3] in which Ta electrodes of 30 nm were used as contact metals. The DNA sequences used are shown in Figure 1. The reporter DNA–AuNP conjugates were synthesized by incubating AuNPs (ca. 1.2 nM) with the reporter DNA (3 μM) in a Tris–ethylenediaminetetraacetate (Tris–EDTA) buffer solution, following a preparation reported elsewhere.[8] The OTS treatment was performed before immobilization of the probe DNA. After immobilization, the SNFETs were further immersed into a PEG solution for 12 h. These blocking procedures, to reduce NSB, are essential for reproducible DNA detection.

A recent report has shown that DNA can be immobilized on SNFETs by physical adsorption,[5] which allows reliable detection of hybridization of complementary DNA. We have also observed that SNFETs immobilized by a DNA molecule encoded with a terminal NH_2 group are reliable for differentiation of its complementary and single-base mismatched DNA analyte.[6] Here we use ''amine-coded probe-DNA'' to carry out the AuNP enhancement study. Figure 2 shows the typical gate voltage (V_g) dependence of the normalized drain current (I_d) for SNFETs, measured at a drain voltage (V_d) of −10 V, where we normalize the I_d at $V_g = -15$ V for the OTS-treated

[*] Dr. S. G. Mhaisalkar, Dr. L. J. Li, Dr. X. C. Dong, Dr. A. Lohani, C. M. Lau
School of Materials Science and Engineering
Nanyang Technological University
50 Nanyang Ave., Singapore 637819 (Singapore)
E-mail: ljli@ntu.edu.sg
Dr. X. C. Dong
Institute of Advanced Materials
Nanjing University of Posts and Telecommunications
9 Wenyuan Road, Nanjing 210046 (PR China)
Dr. Z. X. Shen, J. Kasim
School of Physical and Mathematical Science
Nanyang Technological University
Singapore 637371 (Singapore)
Dr. J. A. Rogers, X. Ho
Department of Materials Science and Engineering
Department of Chemistry
University of Illinois at Urbana–Champaign
Urbana, IL 61801 (USA)

[**] This research was supported by Nanyang Technological University, Singapore.

ADVANCED MATERIALS

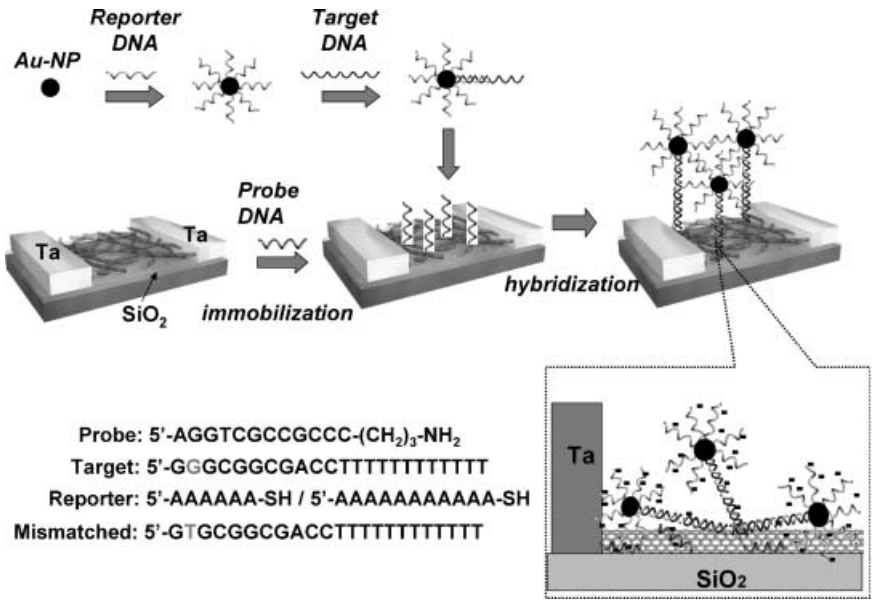

Figure 1. Schematic illustration of DNA detection enhancement by reporter DNA–Au nanoparticle conjugates. The bottom right panel illustrates the possible molecular binding on SWNTs.

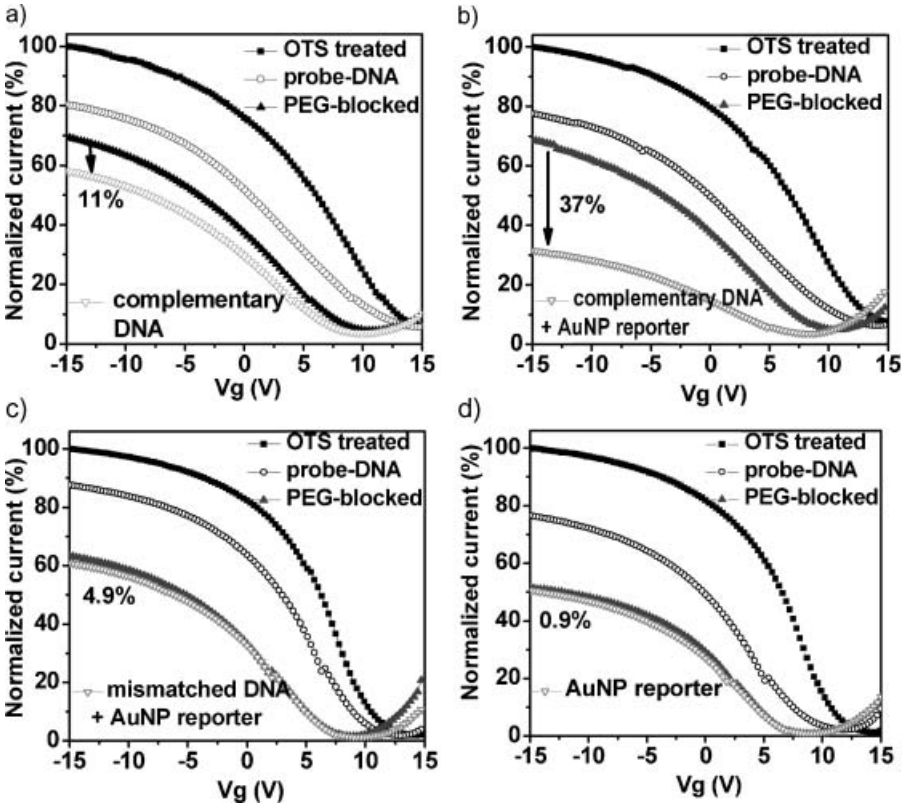

Figure 2. Typical gate voltage dependence of the normalized drain current I_d for SNFETs treated with OTS, immobilized with probe DNA, blocked with PEG and a) hybridized with complementary target DNA, b) hybridized with complementary target DNA and reporter DNA-AuNP conjugates, c) hybridized with single-base mismatched target DNA and reporter DNA–AuNP conjugates, and d) immersed with reporter DNA–Au conjugates. The reporter used for this Figure was 6A DNA. (channel length = 50 μm, $V_d = -10$ V, analyte concentration = 1 nM).

SNFETs. Figure 2a shows that the I_d decreases after immobilization with the probe DNA, and the subsequent PEG blocking further reduces the I_d. In the case without AuNP labeling, 1 nM of complementary DNA results in an I_d decrease of ca. 11%. Figure 2b demonstrates a significant sensing enhancement in detection of complementary DNA, where an I_d decrease of ca. 37% is observed with the participation of 6A reporter DNA–AuNP conjugates. For a direct comparison, Figure 2c shows that an I_d decrease of only ca. 4.9% is observed for the device that forms hybrids with the single-base mismatched DNA (1 nM) encoded with 6A reporter DNA–AuNP conjugates. Figure 2d shows a reference experiment to verify that the reporter–AuNP conjugates alone (without target DNA) do not result in a significant change of I_d. These results suggest that the blocking procedures including OTS and PEG treatments effectively retard NSB from the reporter DNA–AuNP conjugates. Figure 3a summarizes the statistics (based on the sensing results from 7–8 separate devices, 1 nM analyte DNA) in percentage I_d decrease for each case mentioned in Figure 2a–d, where the reporter DNA–AuNP approach amplifies the I_d change from 11% (complementary) to 37% (complementary + AuNP). The decreases of the I_d values derived from the effect of one-base mismatched DNA + 6A reporter DNA–AuNP conjugates (4.8%) or from only 6A reporter DNA–AuNPs (0.9%) are significantly smaller than the decrease derived from AuNP complementary binding trials. Figure 3b compares the correlation between the concentration and percentage I_d decrease for the complementary DNA sensing with the participation of AuNPs conjugated with 6A and 11A reporter DNA individually. The results suggest that 11A reporter DNA induces a larger I_d decrease. The saturation concentration is around 0.1 and 1 nM, respectively, for 11A and 6A reporter DNA. Figure 3b also indicates that a 100 fM complementation DNA detection (ca. 5% I_d change) can be sufficiently differentiated from a 1 nM

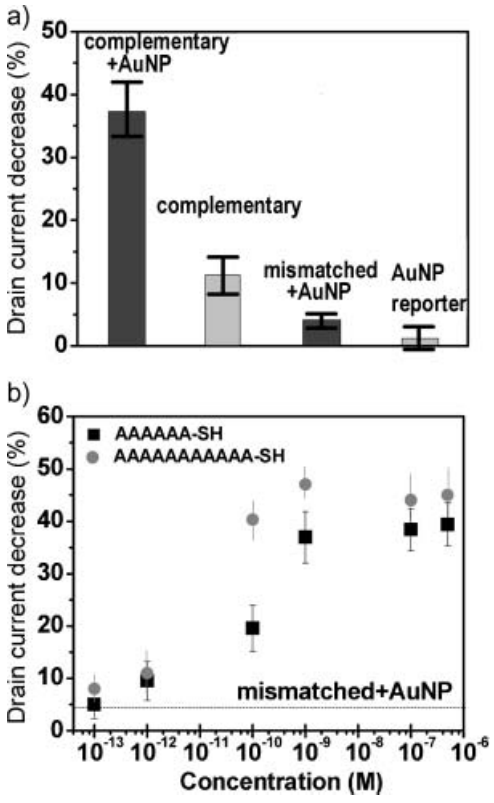

Figure 3. a) Statistics showing the percentage decrease of I_d in SNFETs for various sensing experiments. (The reporter used for this graph is 6A DNA.) b) Percentage I_d decrease versus DNA concentration in the sensing of complementary DNA, enhanced by 6A and 11A reporter DNA–AuNP conjugates. The dashed line shows the limit of selective detection, which is based on the I_d response to the mismatched DNA (1 nM) + 11A reporter DNA–AuNP conjugates.

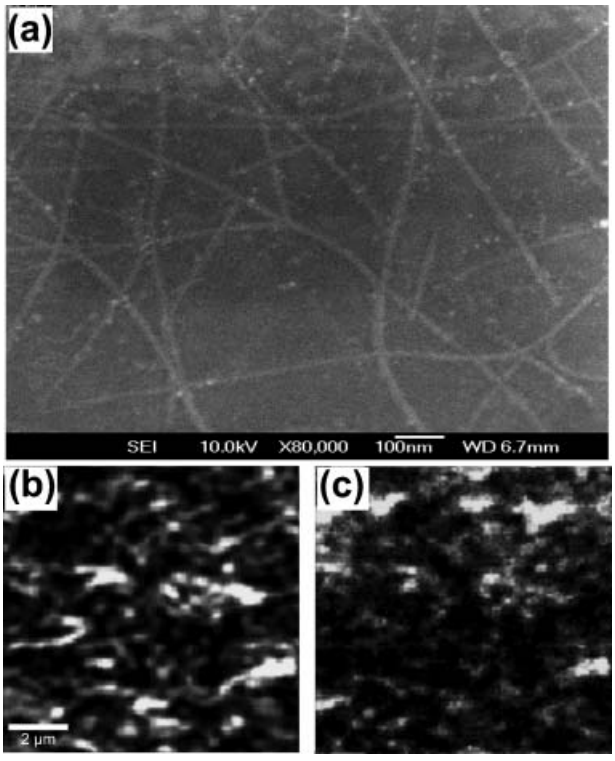

Figure 4. a) SEM image for the SNFET with complementary DNA attached to reporter DNA–AuNP conjugates. The acceleration voltage in the SEM instrument was kept at 10 kV. b) Map of SWNT constructed by integrating the 1530–1640 cm^{-1} region that corresponds to the G-band of the SWNTs in Raman 2D scan. c) Map of AuNPs constructed by integrating the background signal from 1100–1200 cm^{-1} at the same area.

mismatched DNA signal (indicated by the dashed line in Figure 3b).

X-ray photoelectron spectroscopy (XPS) measurements[12] were used to demonstrate that AuNPs are efficiently attached to the SNFETs, where the atomic percentage of P and Au upon hybridization and DNA–AuNP conjugation increases from ''non-detectable'' to 0.29% and 0.38% respectively. The devices used in this study were grown by chemical vapor deposition (CVD) method, and there were some catalytic nanoparticles dispersed on the SiO_2 dielectric before the nanotube growth. Atomic force microscopy (AFM) cannot differentiate the catalytic iron particles from AuNPs. Therefore, scanning electron microscopy (SEM) was used to study the distribution of AuNPs on the device surface. Figure 4a shows a SEM image for the SNFET with complementary DNA attached with reporter DNA–AuNP conjugates. The acceleration voltage in the SEM instrument was kept at 10 kV to observe both SWNT and AuNPs at the same time. We have separately examined that under these imaging conditions, the catalytic particles are not detectable by SEM. Therefore, the SEM result suggests that most of the AuNPs are attached to the SWNTs (the diameter of a SWNT imaged at 10 kV is larger than the real diameter). To further support this argument, we performed 2D Raman scans on the same device. The map of AuNPs can be constructed by integrating the background signal from 1100–1200 cm^{-1} in the confocal Raman measurement, with a typical optical resolution of ca. 0.5 μm. The bright spots in the region indicate an increase in the background continuum signal from metallic nanoparticles (see Supporting Information, Figure S1). Several groups reported that the background enhancement was due to the broad continuum emission from nanoparticles[10–11]. Hence, by observing the increase in the background signal, we are able to locate the gold nanoparticles. Figure 4b and c shows the images for carbon nanotubes (integrating the 1530–1640 cm^{-1} region that corresponds to the G-band of the SWNTs) and that for AuNPs, respectively, at the same area. By comparing these two maps we conclude that most of the AuNPs are attached to SWNTs.

The results thus far are all based on Ta-contacted devices. We have also examined the sensing results using a Au electrode, the work function of which is ca. 5 eV and is commonly used in nanotube devices. We observed that the AuNP-induced enhancement of Au-contacted devices is not as

ADVANCED MATERIALS

pronounced as that of Ta-contacted devices. The AuNP reporter only enhances the I_d reduction for Au-contacted devices from 8% to ca. 12% (data not shown). We believe that the selection of metal electrode is also critical for this approach. Our experimental results could indicate that the Fermi energy difference between electrode and carbon nanotubes may affect the interface change upon addition of AuNP reporters. The detailed mechanism is under investigation.

Based on the transfer curves shown in Figure 2c, the inclusion of reporter DNA–AuNP conjugates induces a negative shift in threshold voltage, indicating that electronic doping from the reporter DNA–AuNP conjugate may contribute to the I_d reduction. This could be explained by that amino functionalities in the reporter DNA may transfer negative charges to carbon nanotubes. It is noted that the channel conduction change induced by doping and scattering centers[5] has been reported to be a co-existent mechanism in DNA detection using SNFETs.[11] However, the reporter DNA–AuNP conjugates induce very different enhancement performances in Ta- and Au-contacted SNFETs, suggesting that the electrode/nanotube interface is significantly affected by the reporter DNA–AuNP conjugates. It has been observed that the sensing of DNA hybridization using SNFETs significantly contributed from the barrier energy change of metal–SWNT junctions.[13–15] Several reports have suggested that short-range dipole (or electrostatic) interactions near the actual electrode–SWNT junction may interact with the junction and, hence, affect the energy level alignment.[16–17] The density of phosphate groups from the DNAs close to the electrode–SWNT junction was believed to be responsible for the change of the electrode/SWNT interface. In this study, this structural reorganization and subsequent junction modulation effect is amplified by the participation of the DNA–AuNP conjugates, thus resulting in increased sensitivity and detection limits for DNA hybridization detection. Figure 1 schematically illustrates the selective binding of reporter DNA–AuNPs with complementary and probe DNA on an SNFET. The AuNPs are attached with a large number of reporter DNAs that provide a very high density of negative charges to the junction, and therefore alter the conductance of the SNFETs. The exact nature of the contribution of the AuNP conjugates is being investigated further by varying the AuNP sizes.

In summary, we have carefully demonstrated a significant sensitivity enhancement in electrical detection of DNA hybridization in SNFETs via the introduction of reporter DNA–AuNP conjugates in the hybridization step. The amplified change in drain current allows us to reliably determine the DNA concentration down to ca. 100 fM. We believe that the device-to-device variation as well as the sensitivity can be further improved by properly adjusting the composition of the SWNT networks (ratio of metallic to semiconducting tubes or ratio between different tube species), which requires further studies in the separation of carbon nanotubes or in the area of selective growth of SWNTs. With detection limits in the femtomolar range, SNFET-based biosensors and immunosensors may be adapted to detection of a variety of biomarkers for applications ranging from molecular diagnostics to in vitro diagnostics.

Experimental

Materials: The Au nanoparticles colloidal suspension (0.01% $HAuCl_4$, particle size 17–23 nm) was purchased from Sigma–Aldrich and used without further purification. The DNA strands used in the experiments were with the sequences: probe DNA: 5′-AGG-TCG-CCG-CCC-$(CH_2)_3$-NH_2; target DNA: 5′-GGG-CGG-CGA-CCT-TTT-TTT- TTT-TT; reporter DNA: 5′-AAA-AAA-SH or AAA-AAA-AAA-AA-SH; and mismatched DNA: 5′-GTG-CGG-CGA-CCT-TTT-TTT-TTT-TT. The following buffer solutions were used: DNA immobilization buffer: Tris–EDTA buffer solution (10 mM Tris-HCl/1.0 mM EDTA/0.10 M NaCl). Hybridization buffer: phosphate buffered saline (PBS, pH 7.4) with 0.25 M NaCl and 10 mM phosphate buffer. All solutions were prepared with MilliQ water (18 MΩ · cm) from a Millipore system.

Fabrication of Carbon Nanotube Transistors: Random networks of SWNTs with diameters between 1 and 3 nm and lengths between 5 and 10 μm were first grown onto SiO_2 (100 nm)/Si wafers using chemical vapor deposition techniques. SWNT network transistors (SNFETs) were fabricated in a top-contact device geometry (illustrated in Scheme 1), where 30 nm of Ta electrodes were patterned on top of it by using standard lithography techniques. The channel lengths of the investigated devices were 50, 75, and 100 μm.

Preparation of Reporter DNA–AuNP Conjugates: The reporter DNA–AuNP conjugates were synthesized by incubating AuNPs (ca. 1.2 nM) with reporter DNA (3 μM) in a Tris–EDTA buffer solution. The Au nanoparticles and reporter DNAs were mixed in a ratio of about 1:2000 (i.e., the number of AuNPs to the number of reporter DNA molecules) to ensure that each AuNP is attached to a large number of reporter DNA strands. Then, the salt concentration was gradually increased to 0.3 M by adding 1 M NaCl solution. After incubation for 20 h, the mixture was centrifuged at 12500 rpm for 60 min. The red oily precipitate was washed, recentrifuged, and finally dispersed in 0.5 mL PBS buffer solution.

Immobilization and Hybridization of DNA: Before immobilization, SNFETs were modified with octyltrichlorosilane (OTS) to remove the possible adsorption of DNA on SiO_2 substrate by blocking the surface Si–OH bonds. SNFETs were then immersed in 1 μM probe DNA in Tris–EDTA buffer solution for a period of 16–24 h. A standard rinsing with Tris–EDTA buffer was performed to remove the weakly bound DNA, and SNFETs were blown dry before electrical characterization. After immobilization, SNFETs were immersed in an 80% polyethylene glycol (PEG, molecular weight 380–420) aqueous solution for 12 h to block the vacant SWNT surface, then rinsed with water and followed by blow drying. For hybridization, 10 μL DNA solutions (target DNA with or without reporter DNA–AuNPs, or mismatch DNA) were pipetted onto the immobilized SNFETs for 1 h, followed by washing and drying.

Raman Measurements: The Raman microscopy setup was based on a WITec CRM200 confocal Raman microscopy system (50 μm pinhole) with an OLYMPUS microscope objective (100×, NA = 0.95). A double-frequency Nd:YAG laser (532 nm, 100 mW, CNI Laser) was used as the excitation source. The laser was coupled into a 3.5 μm core diameter single-mode fiber. The linearly polarized Gaussian beam (TEM_{00}) was used to excite the Raman signal. The sample was put on a translation stage, which could be moved coarsely along the *x*- and *y*-axes. It could also be finely moved with a piezostage. The piezostage had travel distances of 100 μm along the *x*- and *y*-directions and 20 μm in the *z*-direction. The Raman scattered light was directed to a 600 grooves mm^{-1} grating and detected using a TE-cooled charge-coupled device (CCD) cooled to −64 °C.

XPS and Electrical Measurements: The samples for XPS measurement, SWNT on SiO_2, were incubated in 1 μM probe DNA solution for a period of 16 h, followed by washing and drying with N_2. Another fresh

sample (SWNTs on SiO_2) was immobilized with probe DNA and then hybridized with 10 μL target DNA (100 nM) with reporter DNA–AuNPs for 1 h, followed by washing and drying with N_2 before XPS testing. XPS measurements were carried with a Kratos AXIS spectrometer (UK) with monochromatic Al Kα X-ray radiation at 1486.71 eV. The base vacuum in XPS analysis chamber was about 1×10^{-9} Torr ($1\,\text{Torr} = 1.333 \times 10^2$ Pa). All spectra were calibrated using C 1s at 284.6 eV as a reference. Pass energy was kept at 40 eV and the step size 0.1 eV. Data acquisition, processing, and quantification were done with the Kratos Vision Processing 2.1.3. All electrical measurements were carried out in ambient using a Keithley semiconductor parameter analyzer Model 4200-SCS.

Received: November 10, 2007
Revised: February 5, 2008
Published online: May 19, 2008

[1] E. S. Snow, J. P. Novak, P. M. Campbell, D. Park, *Appl. Phys. Lett.* **2003**, *82*, 2145.
[2] K. Bradley, J. C. Gabriel, G. Gruner, *Nano Lett.* **2003**, *3*, 1353.
[3] a) S. H. Hur, D. Y. Khang, C. Kocabas, J. A. Rogers, *Appl. Phys. Lett.* **2004**, *85*, 5730. b) Y. Zhou, A. Gaur, S. H. Hur, C. Kocabas, M. Meitl, M. Shim, J. A. Rogers, *Nano Lett.* **2004**, *4*, 2031.
[4] C. W. Lee, K. Zhang, H. Tantang, A. Lohani, T. Nagahiro, K. Tamada, Y. Chen, S. G. Mhaisalkar, L. J. Li, *Appl. Phys. Lett.* **2007**, *91*, 103515.
[5] A. Star, E. Tu, J. Niemann, J.-C. P. Gabriel, C. S. Joiner, Christian Valcke, *Proc. Natl. Acad. Sci. USA* **2006**, *103*, 921.
[6] E. L. Gui, L. J. Li, P. S. Lee, A. Lohani, S. G. Mhaisalkar, Q. Cao, J. Kang, J. A. Rogers, N. C. Tansil, Z. Gao, *Appl. Phys. Lett.* **2006**, *89*, 232104.
[7] J. A. Hansen, R. Mukhopadhyay, J. Hansen, K. V. Gothelf, *J. Am. Chem. Soc.* **2006**, *128*, 3860.
[8] J. Zhang, S. Song, L. Zhang, L. Wang, H. Wu, D. Pan, C. Fan, *J. Am. Chem. Soc.* **2006**, *128*, 8575.
[9] S. I. Tanaka, M. Taniguchi, T. Kawai, *Japan. J. Appl. Phys.* **2004**, *43*, 7346.
[10] Y. C. Cao, R. Jin, C. A. Mirkin, *Science* **2002**, *297*, 1536.
[11] A. M. Michaels, M. Nirmal, L. E. Brus, *J. Am. Chem. Soc.* **1999**, *121*, 9932.
[12] XPS results (1) before hybridization: C 54.32%; N 1.76%; O 43.92%; P and Au: lower than detection limit; (2) after hybridization with AuNP enhancement: C 65.43%; N 3.41%; O 30.48%; P 0.29%; Au 0.38%.
[13] E. L. Gui, L. J. Li, K. Zhang, Y. Xu, X. Dong, X. Ho, P. S. Lee, J. Kasim, Z. X. Shen, J. A. Rogers, S. G. Mhaisalkar, *J. Am. Chem. Soc.* **2007**, *129*, 14428.
[14] X. Tang, S. Bansaruntip, N. Nakayama, E. Yenilmez, Y. I. Chang, Q. Wang, *Nano Lett.* **2006**, *6*, 1632.
[15] R. J. Chen, H. C. Choi, S. Bansaruntip, E. Yenilmez, X. Tang, Q. Wang, Y. L. Chang, H. Dai, *J. Am. Chem. Soc.* **2004**, *126*, 1563.
[16] N. D. Lang, Ph, Avouris, *Nano Lett.* **2002**, *2*, 1047.
[17] X. Cui, M. Freitag, R. Martel, L. Brus, Avouris. Ph, *Nano Lett.* **2003**, *6*, 783.

